Title

Polarization effects in AlGaN/GaN and GaN/AlGaN/GaN heterostructures

Journal

Journal of Applied Physics, 93(12)

ISSN

0021-8979

Authors

Heikman, S

Keller, S

Wu, Y

et al.

Publication Date

2003-06-01

Peer reviewed

Polarization effects in AlGaN/GaN and GaN/AlGaN/GaN heterostructures

Sten Heikman,[a] Stacia Keller, Yuan Wu, James S. Speck, Steven P. DenBaars, and Umesh K. Mishra
Department of Electrical and Computer Engineering and Materials Department, University of California, Santa Barbara, California 93106

(Received 18 February 2003; accepted 2 April 2003)

The influence of AlGaN and GaN cap layer thickness on Hall sheet carrier density and mobility was investigated for $Al_{0.32}Ga_{0.68}N$/GaN and GaN/$Al_{0.32}Ga_{0.68}N$/GaN heterostructures deposited on sapphire substrates. The sheet carrier density was found to increase and saturate with the AlGaN layer thickness, while for the GaN-capped structures it decreased and saturated with the GaN cap layer thickness. A relatively close fit was achieved between the measured data and two-dimensional electron gas densities predicted from simulations of the band diagrams. The simulations also indicated the presence of a two-dimensional hole gas at the upper interface of GaN/AlGaN/GaN structures with sufficiently thick GaN cap layers. A surface Fermi-level pinning position of 1.7 eV for AlGaN and 0.9–1.0 eV for GaN, and an interface polarization charge density of 1.6×10^{13}–1.7×10^{13} cm^{-2}, were extracted from the simulations. © *2003 American Institute of Physics.* [DOI: 10.1063/1.1577222]

I. INTRODUCTION

AlGaN/GaN based high electron mobility transistors have demonstrated great potential for high-power high-frequency applications, with breakdown voltages in excess of 1 kV,[1] and microwave power densities higher than 11 W/mm at 10 GHz.[2] A high sheet carrier density two-dimensional electron gas (2DEG) can be formed at the AlGaN/GaN interface, without intentional doping of the structure. The polarization along the (0001) axis of the (Al)GaN crystal is the key factor determining the band structure and charge distribution in the heterostructure.[3] The difference in spontaneous and piezoelectric polarization between AlGaN and GaN effectively results in a fixed sheet of polarization charge at the AlGaN/GaN interface. This polarization charge is positive for structures grown on Ga-polar GaN, and serves to attract high concentrations of electrons. The origin of the electrons is uncertain, however, the most plausible model to date, proposed by Ibbetson *et al.*,[4] suggests that the electrons originate from donorlike states on the AlGaN surface.

Analogous to the formation of a 2DEG at an AlGaN/GaN interface, a two-dimensional hole gas (2DHG) can form at an AlGaN/GaN interface with a negative polarization charge.[5–7] Such interfaces are present in AlGaN/GaN single heterostructures on N-polar GaN, and in GaN/AlGaN/GaN structures on Ga-polar GaN, at the upper GaN/AlGaN interface. The formation of 2DHGs has been observed experimentally for Mg-doped GaN/AlGaN/GaN structures and AlGaN/GaN superlattices.[8–10]

A detailed understanding of the heterostructure band diagrams, charge distribution, and surface effects, is essential for further developments in device designs. In this article, a comprehensive study of $Al_{0.32}Ga_{0.68}N$/GaN and GaN/$Al_{0.32}Ga_{0.68}N$/GaN heterostructures is reported. Observed changes in the sheet carrier density, in response to variations in AlGaN and GaN layer thicknesses, are analyzed and correlated to simulations of the band diagrams. Both the concept of a pinned Fermi level at the surface, and the formation of a 2DHG at the upper interface of some GaN/AlGaN/GaN structures, are invoked in the analysis. In fitting the simulated 2DEG sheet charge densities to the experimental values, good fits were achieved, and values for the interface polarization charge and the Fermi-level surface pinning position, used as fitting parameters, were extracted.

II. EXPERIMENT

The samples were grown by metalorganic chemical vapor deposition (MOCVD) using the precursors trimethylaluminum, trimethylgallium, and ammonia. The AlGaN/GaN layer structures were grown on 3 μm semi-insulating GaN base layers, prepared on sapphire substrates. The base layers were rendered semi-insulating by Fe doping of the first 0.7 μm of growth.[11] The AlGaN was grown under the following conditions: 1040 °C growth temperature, 100 Torr total pressure, 25 Torr ammonia partial pressure, and a growth rate of 0.8 Å/s. The growth conditions for the thin (<20 nm) GaN cap layers were the same, except for a lower growth rate of 0.5 Å/s. For the structures with a thick GaN cap layer, the GaN growth was performed at atmospheric pressure, at a growth rate of 6 Å/s.

Three series of heterostructures were grown and, in each series, the thickness of one layer was varied. One series consisted of single AlGaN/GaN heterostructures, with varied AlGaN thickness, and two series consisted of GaN/AlGaN/GaN heterostructures, with either the AlGaN thickness varied, or the GaN cap layer thickness varied.

Hall effect measurements were performed in the van der Pauw geometry, on cleaved 6 mm×6 mm squares, using In contacts. The samples were generally measured within a few

[a]Electronic mail: sten@ece.ucsb.edu

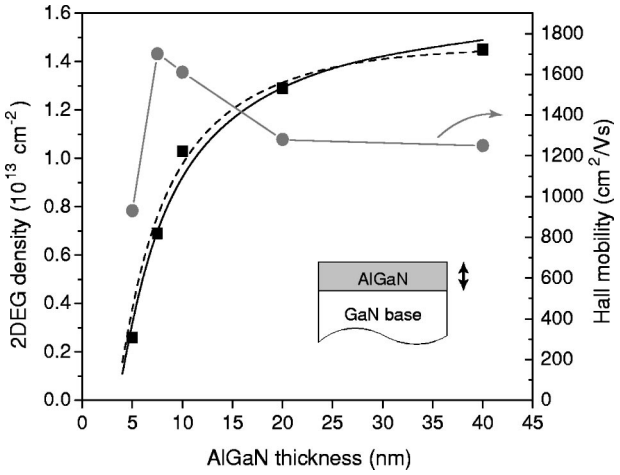

FIG. 1. The influence of AlGaN thickness on sheet carrier density and Hall mobility, for AlGaN/GaN single heterostructure. The black lines are simulation fits; the solid line assuming no point defects in the structure, the dashed line using a shallow acceptor concentration in the AlGaN layer as a fitting parameter. The gray line is a guide for the eyes.

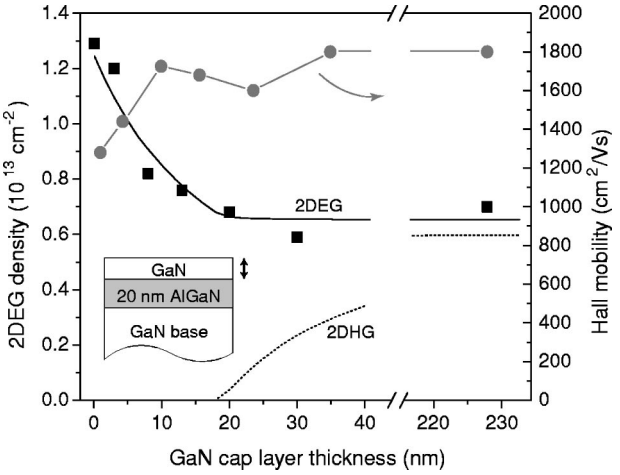

FIG. 2. The effect of GaN cap layer thickness on sheet carrier density and Hall mobility, for a GaN/AlGaN/GaN heterostructure with a fixed AlGaN layer thickness of 20 nm. The black solid line is a fit to simulations, and the gray line connecting the Hall mobility points is a guide for the eyes.

hours of finishing the growth, to avoid aging effects. The Al composition, which was 32% throughout the study, and the growth rates, were deduced from x-ray diffraction measurements of an AlGaN/GaN superlattice calibration sample. The material quality was further assessed by transmission electron microscopy (TEM) and secondary ion mass spectrometry (SIMS).

Simulations of the band diagram and the free carrier distribution of the heterostructures were performed with a self-consistent one-dimensional Schrödinger–Poisson solver.[12] The following material parameters were used: The band gap of $Al_xGa_{1-x}N$ at room temperature given by $E_g(x) = x6.2\ \text{eV} + (1-x)3.4\ \text{eV} - x(1-x)1.0\ \text{eV}$, conduction-band offset $\Delta E_C = 0.7[E_g(x) - E_g(0)]$,[13,14] and dielectric constant $\epsilon_r(x) = 8.9 - 0.4x$.[15,16] The effect of exchange correlation on Coulomb interaction was neglected, as this has been shown not to affect sheet carrier densities in AlGaN/GaN heterostructures.[17] The background donor concentration of the GaN and AlGaN layers was set to zero, based on SIMS observations, and on resistivity measurements of nominally undoped GaN grown in our reactor.[11]

III. RESULTS

In the first series of heterostructures, single $Al_{0.32}Ga_{0.68}N$ layers were deposited on semi-insulating GaN base layers, and the AlGaN thickness was varied between 5 nm and 40 nm. Figure 1 shows the resulting sheet carrier density and Hall mobility, as a function of the AlGaN thickness. Between 5 nm and 10 nm, the sheet carrier density increased rapidly from 2.6×10^{12} cm^{-2} to 1.03×10^{13} cm^{-2}. However, beyond 10 nm, the sheet carrier density increased slower, reaching 1.45×10^{13} cm^{-2} for a thickness of 40 nm. The Hall mobility showed the opposite trend to the sheet carrier density, for AlGaN thicknesses above 5 nm, with values decreasing from 1700 cm^2/V s at 7.5 nm, down to 1250 cm^2/V s at 40 nm.

The second series consisted of GaN/AlGaN/GaN heterostructures, with a GaN cap layer thickness varying between 3 nm and 228 nm, and a fixed AlGaN layer thickness of 20 nm. The resulting sheet carrier densities and Hall mobilities are plotted in Fig. 2, as a function of the GaN cap layer thickness. The presence of the GaN cap layer resulted in a reduction of the sheet carrier density, from 1.29×10^{13} cm^{-2} with no GaN cap, down to 5.9×10^{12} cm^{-2} with a 30 nm cap layer. For a 228 nm thick GaN cap layer, the sheet carrier density was 7×10^{12} cm^{-2}. It was observed that the samples with GaN cap layers of thickness between 13 nm and 30 nm were sensitive to the measurement conditions. For a probe current of 0.1 mA, the measured sheet carrier densities decreased during consecutive measurements, in some cases up to 30%. The effect was reduced for lower probe currents. The Hall mobilities roughly followed the same trend as was observed for the first series, with increasing values for decreasing sheet carrier densities.

In the third series, the GaN cap layer thickness was kept constant at 228 nm, while the AlGaN layer thickness was varied between 20 nm and 50 nm. Figure 3 shows the resulting sheet carrier density and Hall mobility, as a function of the AlGaN thickness. The sheet carrier density increased with increasing AlGaN thickness, from 7×10^{12} cm^{-2} for 20 nm AlGaN thickness to 1.24×10^{13} cm^{-2} for 50 nm AlGaN thickness. Again, as was observed in the previous two series, the Hall mobility decreased as the sheet carrier density increased. TEM was performed on the sample with 50 nm AlGaN thickness to confirm that the AlGaN layer and the GaN cap layer were fully strained to the underlying GaN base layer. The resulting cross-sectional TEM image, Fig. 4, shows negligible relaxation and no additional extended defects generated in the AlGaN layer or in the GaN cap layer.

SIMS investigations were performed, monitoring the standard impurities, on a sample with 50 nm buried $Al_{0.32}Ga_{0.68}N$ and GaN layers, grown under conditions identical to the low growth-rate layers in the measured heterostructures. Impurity concentrations of 2.2×10^{17} cm^{-3} carbon, 1.7×10^{17} cm^{-3} oxygen, and 4×10^{16} cm^{-3} silicon, were detected in the AlGaN layer, while the GaN layer showed impurity concentrations of 5×10^{16} cm^{-3} carbon, 8

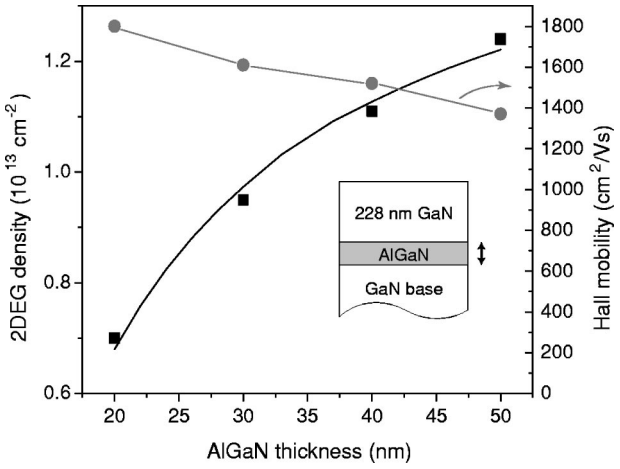

FIG. 3. The influence of AlGaN layer thickness on sheet carrier density and Hall mobility, for a GaN/AlGaN/GaN heterostructure with a fixed GaN cap layer thickness of 228 nm. The black solid line is a fit to simulations, and the gray line connecting the Hall mobility points is a guide for the eyes.

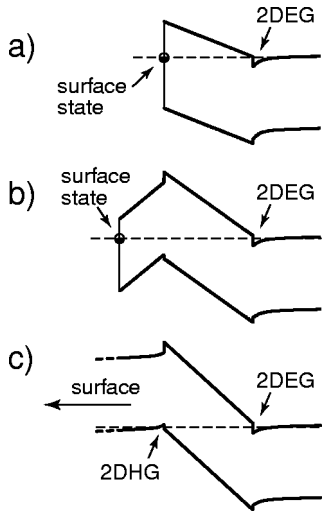

FIG. 5. Band diagrams of three heterostructures: (a) single AlGaN/GaN heterostructure, (b) GaN/AlGaN/GaN heterostructure with a *thin* GaN cap, and (c) GaN/AlGaN/GaN heterostructure with a *thick* GaN cap.

$\times 10^{15}$ cm^{-3} silicon, and an oxygen concentration below the detection limit.

IV. DISCUSSION

The increase and saturation of charge with AlGaN thickness in AlGaN/GaN single heterostructures has previously been reported for samples grown by both MOCVD and molecular-beam epitaxy (MBE), for various Al compositions.[4,18–21] Furthermore, the decrease and saturation of charge with the thickness of a GaN cap layer has been observed in GaN/AlN/GaN structures.[22]

To understand the observed trends, the band diagrams of the heterostructures were simulated, and the resulting sheet carrier densities were fitted to the experimental data. In modeling the band diagrams, the Fermi level was assumed to be pinned by donorlike states at the surface, at an energy E_D below the conduction-band minimum. This assumption was based on experimental observations of surface pinning,[20,21,23–26] and on previous modeling of AlGaN/GaN single heterostructures.[4,18,19] E_D was assumed independent of the GaN and/or AlGaN layer thicknesses, but different values were allowed for GaN and $Al_{0.32}Ga_{0.68}N$ surfaces. Figure 5 illustrates band diagrams representative of the three experimental series: A single AlGaN/GaN heterostructure [Fig. 5(a)], a GaN/AlGaN/GaN heterostructure with a thin GaN cap [Fig. 5(b)], and a GaN/AlGaN/GaN heterostructure with a thick GaN cap [Fig. 5(c)]. The polarization charge was modeled as a fixed positive sheet charge $+\sigma_{pz}$ at the lower AlGaN/GaN interface, and as a fixed negative sheet charge $-\sigma_{pz}$ of equal magnitude at the upper GaN/AlGaN interface for the samples with a GaN cap layer. The values of E_D and σ_{pz} were both used as fitting parameters.

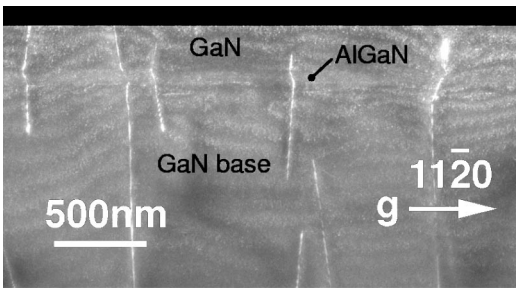

FIG. 4. Cross-sectional weak beam TEM image of $GaN/Al_{0.32}Ga_{0.68}N/GaN$ structure, with 50 nm AlGaN layer thickness. The image shows negligible strain relaxation in the AlGaN layer.

The simulated 2DEG sheet charge density of the AlGaN/GaN single heterostructure, included in Fig. 1 as a solid line, showed close agreement to the measured data with $E_D = 1.7$ eV and $\sigma_{pz} = 1.69 \times 10^{13}$ cm^{-2}. When introducing a shallow acceptor concentration N_a in the AlGaN layer as a third fitting parameter, a slightly better fit could be achieved, with the values $E_D = 1.7$ eV, $\sigma_{pz} = 1.78 \times 10^{13}$ cm^{-2}, and $N_a = 7 \times 10^{17}$ cm^{-3} (included in Fig. 1 as a dashed line). The nature of a possible shallow acceptor is unclear; SIMS investigations showed that the standard impurities C, O, and Si, were low, but other impurities, or native defects, could possibly account for the acceptor concentration.

Adding a GaN cap layer to the AlGaN/GaN structure introduced a negative polarization charge at the upper heterointerface, causing increased electric fields in the AlGaN, and a decrease in 2DEG density [illustrated in Fig. 5(b)]. As the GaN cap layer thickness increased, the valence-band shifted upward, eventually reaching the Fermi level. At this point, a 2DHG formed at the upper GaN/AlGaN interface, pinning the valence band, hindering any further increase of the electric field in the AlGaN layer [Fig. 5(c)]. The predicted decrease and saturation in 2DEG sheet charge density was observed in the measured Hall data in Fig. 2. The best fit of the simulated data to the experimental data was achieved with the values $E_D = 0.9$–1.0 eV and $\sigma_{pz} = 1.58 \times 10^{13}$ cm^{-2}. The predicted 2DHG sheet charge density is also included in Fig. 2 as a dotted line. In samples with a 2DHG formed next to the 2DEG, it may at first seem that both the 2DEG and the 2DHG would be probed by Hall effect measurements. However, due to a much superior mo-

bility and conductance of the 2DEG compared to the 2DHG, nearly all of the probing current flows through the 2DEG, with the effect that the measured sheet carrier density and mobility are completely dominated by the 2DEG.

In the series of samples with thick GaN-capped GaN/AlGaN/GaN structures, the surface effects were removed from the two-dimensional carrier gasses. The GaN on both sides of the AlGaN had nearly flat bands [see Fig. 5(c)], and the 2DHG and 2DEG sheet charge densities were nearly equal in magnitude. In the simulations, the choice of E_D had a negligible effect on the 2DEG sheet charge density. The pinning of the valence band at the 2DHG screened the 2DEG from changes in the electric field in the GaN cap layer. Moreover, the high thickness of the cap layer ensured that changes in E_D caused only low electric-field changes in the cap layer. For example, a 1 V change in E_D resulted in a 45 kV/cm change in the electric field, which is less than 5% of the field present in the AlGaN layer. The simulations also showed that as the AlGaN thickness was increased, the electric field in the AlGaN was reduced, accompanied by an increase in the 2DEG and 2DHG sheet charge densities. The optimum fit to the experimental data, included as a solid line in Fig. 3, was obtained with a polarization of $\sigma_{pz}=1.60\times10^{13}$ cm^{-2}.

The extracted values of the interfacial polarization charge density σ_{pz} ranged from 1.58×10^{13} cm^{-2} to 1.69×10^{13} cm^{-2} in the three series, assuming no shallow acceptors in the AlGaN. These values are higher than an earlier report from a similar experiment on $Al_{0.34}Ga_{0.66}N$/GaN structures, $\sigma_{pz}=1.46\times10^{13}$ cm^{-2},[4] and higher than those determined by *ab inito* calculations by Fiorentini *et al.*[27] accounting for alloy polarization nonlinearity, $\sigma_{pz}=1.44\times10^{13}$ cm^{-2}. However, close agreement is found to interface polarization extracted from a recent study using capacitance–voltage profiling, where an extrapolated empirical fit gave a value of $\sigma_{pz}=1.64\times10^{13}$ cm^{-2} for an $Al_{0.32}Ga_{0.68}N$/GaN interface.[28]

The experimentally inferred values of the Fermi-level surface pinning position E_D were 1.7 eV and 0.9–1.0 eV, for $Al_{0.32}Ga_{0.68}N$ and a GaN surfaces, respectively. The AlGaN value is within the range of reported values; 1.65 eV has previously been extracted from a similar experiment on $Al_{0.34}Ga_{0.66}N$/GaN structures,[4] and x-ray photoelectron spectroscopy studies have yielded values of $E_D\sim1.6$ eV for $Al_{0.24}Ga_{0.76}N$/GaN samples,[21] and $E_D=1.3$ eV for an $Al_{0.41}Ga_{0.59}N$ surface.[24] For GaN surfaces, there is a wider range of reported values; studies by x-ray photoelectron spectroscopy have yielded values of $E_D\sim1.4$ eV (Ref. 23) and $E_D=1.0$ eV (Ref. 25) for GaN grown by MOCVD, and $E_D\sim0.3$ eV for GaN grown by MBE.[26] Furthermore, $E_D=0.7$ eV has been measured by scanning Kelvin probe microscopy of unintentionally doped GaN.[20] The large variation is probably related to various chemical contaminations of the surface layer, including adsorption of ionic species on the sample surface.[29]

The sensitivity of the simulations to changes in the fitting parameters is illustrated in Fig. 6, for the case of the single $Al_{0.32}Ga_{0.68}N$/GaN heterostructure. The shaded areas represent the change in the simulated sheet carrier density, in response to a $\pm10\%$ variation of the Fermi-level surface pinning position E_D (left-hand side) and to a $\pm10\%$ variation of the interfacial polarization charge σ_{pz} (right-hand side) around the best-fit values. The sheet carrier density is relatively insensitive to variations in E_D, but it is sensitive to σ_{pz}, which means that the experimentally inferred value of E_D has some uncertainty, while the values for σ_{pz}, ranging from 1.58×10^{13} cm^{-2} to 1.69×10^{13} cm^{-2}, are more accurate.

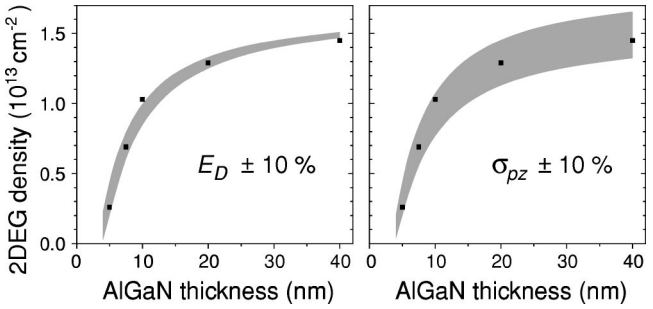

FIG. 6. The sensitivity of the simulated sheet carrier density of a single $Al_{0.32}Ga_{0.68}N$/GaN heterostructure to variations in E_D and σ_{pz}. The experimental values are included as squares.

In the modeling of the heterostructures, the surface Fermi-level position was assumed independent of the layer thicknesses, and the assumption was validated by a relatively good fit to the experimental data. In literature, both a fixed surface pinning position, measured by x-ray photoelectron spectroscopy,[21] and a varying surface Fermi level, measured by scanning Kelvin probe microscopy,[20] have been reported.

V. CONCLUSIONS

In conclusion, AlGaN/GaN and GaN/AlGaN/GaN pseudomorphically strained heterostructures were grown, and the 2DEG sheet charge density, as measured by Hall effect measurements, was studied as a function of the layer thicknesses. The sheet carrier density was found to increase and saturate with the AlGaN layer thickness, while the presence of a GaN cap layer caused a decrease in the charge until saturation. A relatively close fit was achieved between the measured data and 2DEG sheet charge densities obtained from simulations of the band diagrams. The simulations also indicated the presence of a 2DHG at the upper interface of GaN/AlGaN/GaN structures with sufficiently thick GaN cap layers. A surface Fermi-level pinning position of 1.7 eV for AlGaN and 0.9–1.0 eV for GaN, and an interface polarization charge between 1.58×10^{13} cm^{-2} and 1.69×10^{13} cm^{-2}, were extracted from the simulations.

ACKNOWLEDGMENTS

The authors gratefully acknowledge the support of the Air Force Office of Scientific Research, through a contract monitored by Dr. Gerald Witt, and the support of the Office of Naval Research through the Center for Advanced Nitride Electronics (CANE), monitored by Dr. Harry Dietrich. The work also made use of the MRL Central Facilities supported by the National Science Foundation under Award No. DMR96-32716.

[1] N. Q. Zhang, B. Moran, S. P. DenBaars, U. K. Mishra, X. W. Wang, and T. P. Ma, Phys. Status Solidi A **188**, 213 (2001).
[2] J. R. Shealy, V. Kaper, V. Tilak, T. Prunty, J. A. Smart, B. Green, and L. F. Eastman, J. Phys.: Condens. Matter **14**, 3499 (2002).
[3] O. Ambacher *et al.*, J. Appl. Phys. **87**, 334 (2000).
[4] J. P. Ibbetson, P. T. Fini, K. D. Ness, S. P. DenBaars, J. S. Speck, and U. K. Mishra, Appl. Phys. Lett. **77**, 250 (2000).
[5] L. Hsu and W. Walukiewicz, Appl. Phys. Lett. **74**, 2405 (1999).
[6] M. S. Shur, A. D. Bykhovski, and R. Gaska, Solid-State Electron. **44**, 205 (2000).
[7] S. Hackenbuchner, J. A. Majewski, G. Zandler, and P. Vogl, J. Cryst. Growth **230**, 607 (2001).
[8] A. Link, O. Ambacher, I. P. Smorchkova, U. K. Mishra, J. S. Speck, and M. Stutzmann, Mater. Sci. Forum **353**, 787 (2000).
[9] P. Kozodoy, M. Hansen, S. P. DenBaars, and U. K. Mishra, Appl. Phys. Lett. **74**, 3681 (1999).
[10] K. Kumakura and N. Kobayashi, Jpn. J. Appl. Phys., Part 2 **38**, L1012 (1999).
[11] S. Heikman, S. Keller, S. P. DenBaars, and U. K. Mishra, Appl. Phys. Lett. **81**, 439 (2002).
[12] G. L. Snider (1D Poisson/Schrödinger: A Band Diagram Calculator, University of Notre Dame, 1996).
[13] G. Martin, S. Strite, A. Botchkarev, A. Agarwal, A. Rockett, H. Morkoç, W. R. L. Lambrecht, and B. Segall, Appl. Phys. Lett. **65**, 610 (1994).
[14] G. Martin, A. Botchkarev, A. Rockett, and H. Morkoç, Appl. Phys. Lett. **68**, 2541 (1996).
[15] S. N. Mohammad and H. Morkoç, Prog. Quantum Electron. **20**, 361 (1996).
[16] V. W. L. Chin, T. L. Tansley, and T. Osotchan, J. Appl. Phys. **75**, 7365 (1994).
[17] B. Jogai, J. Appl. Phys. **91**, 3721 (2002).
[18] I. P. Smorchkova, C. R. Elsass, J. P. Ibbetson, R. Vetury, B. Heying, P. Fini, E. Haus, S. P. DenBaars, J. S. Speck, and U. K. Mishra, J. Appl. Phys. **86**, 4520 (1999).
[19] C. R. Elsass *et al.*, Jpn. J. Appl. Phys., Part 1 **40**, 6235 (2001).
[20] G. Koley and M. G. Spencer, J. Appl. Phys. **90**, 337 (2001).
[21] H. W. Jang, C. M. Jeon, K. H. Kim, J. K. Kim, S. B. Bae, J. H. Lee, J. W. Choi, and J. L. Lee, Appl. Phys. Lett. **81**, 1249 (2002).
[22] I. P. Smorchkova, L. Chen, T. Mates, L. Shen, S. Heikman, B. Moran, S. Keller, S. P. DenBaars, J. S. Speck, and U. K. Mishra, J. Appl. Phys. **90**, 5196 (2001).
[23] T. Hashizume, S. Ootomo, S. Oyama, M. Konishi, and H. Hasegawa, J. Vac. Sci. Technol. B **19**, 1675 (2001).
[24] A. Rizzi and H. Lüth, Appl. Phys. A: Mater. Sci. Process. **75**, 69 (2002).
[25] A. Rizzi, Appl. Surf. Sci. **190**, 311 (2002).
[26] M. Kočan, A. Rizzi, H. Lüth, S. Keller, and U. K. Mishra, Phys. Status Solidi B **234**, 773 (2002).
[27] V. Fiorentini, F. Bernardini, and O. Ambacher, Appl. Phys. Lett. **80**, 1204 (2002).
[28] E. J. Miller, E. T. Yu, C. Poblenz, C. Elsass, and J. S. Speck, Appl. Phys. Lett. **80**, 3551 (2002).
[29] R. Neuberger, G. Müller, O. Ambacher, and M. Stutzmann, Phys. Status Solidi A **185**, 85 (2001).